Mar Geophys Res (2011) 32:299–311
DOI 10.1007/s11001-011-9131-3

ORIGINAL RESEARCH PAPER

The eastern slope of the southern Adriatic basin: a case study of submarine landslide characterization and tsunamigenic potential assessment

A. Argnani · S. Tinti · F. Zaniboni · G. Pagnoni · A. Armigliato · D. Panetta · R. Tonini

Received: 9 April 2010 / Accepted: 2 April 2011 / Published online: 19 April 2011

Abstract The southern Adriatic basin is the current foredeep of the Albanide fold-and-thrust belt that runs along the eastern boundary of the Adriatic basin and partly owes its remarkable water depth, deeper than 1,000 m, to the Mesozoic palaeogeography of the region. The eastern slope of the southern Adriatic basin is characterized by a thick stack of sedimentary prograding units, fed by sediments coming from the adjacent fold-and-thrust belt, which is still seismically active (e.g. 1979 Montenegro, M = 6.8). This slope presents extensive evidence of large-scale mass wasting throughout its Quaternary evolution and appears as a destructive slope system affected by progressive retreat. A submarine slide located along the eastern slope of the southern Adriatic basin has been recently characterized with good detail. The slide is of relatively small volume (0.031 km^3) and shows a limited displacement, without major internal disruption. The small volume of the landslide combined with its relatively large water depth (headscarp at about 560 m and deposit at 700 m) result in a limited tsunamigenic potential, that has been assessed numerically by means of a Lagrangian block model as regards the slide motion and through a shallow-water finite-difference code for the tsunami waves propagation. Despite the almost negligible tsunami effects, the studied landslide can be taken as a lower case limit for other events along the scarp, and the observed features concerning the generated wave and its impact on the coast can be considered valid also for bigger events.

Keywords Submarine landslide · Tsunami modelling · Destructive slope system · Southern Adriatic basin · Bathymetry

Introduction

The southern Adriatic basin is a sub-circular depression, more than 1,000 m deep, located between the coasts of Apulia, to the west, and Albania, Montenegro and Croatia to the east (Fig. 1).

A recently acquired multibeam bathymetry along the eastern slope of the southern Adriatic basin shows that the slope presents extensive evidence of large-scale mass wasting throughout its Late Quaternary evolution (Argnani et al. 2006). The eastern slope of the southern Adriatic basin, therefore, appears as a destructive slope system affected by progressive retreat, which is mainly due to mass wasting processes.

The anatomy of one of the submarine slides distributed along the eastern slope of the southern Adriatic basin has been recently characterized with some details, thanks to multibeam bathymetry and chirp sonar profiles. This landslide deposit has a relatively small volume and shows a limited displacement, without major internal disruption.

By using these sets of information the geometry of the sliding body has been reconstructed, its volume estimated (0.031 km^3) and the tsunamigenic potential modelled. In addition, some expedite methods available in the literature to estimate the slide volume have been used for comparison.

A. Argnani · D. Panetta
ISMAR-CNR, Istituto di Scienze Marine, Sede di Bologna, Via Gobetti 101, 40129 Bologna, Italy

S. Tinti · F. Zaniboni (✉) · G. Pagnoni · A. Armigliato · R. Tonini
Department of Physics, Sector of Geophysics, University of Bologna, Viale Carlo Berti Pichat 8, 40127 Bologna, Italy
e-mail: filippo.zaniboni@unibo.it

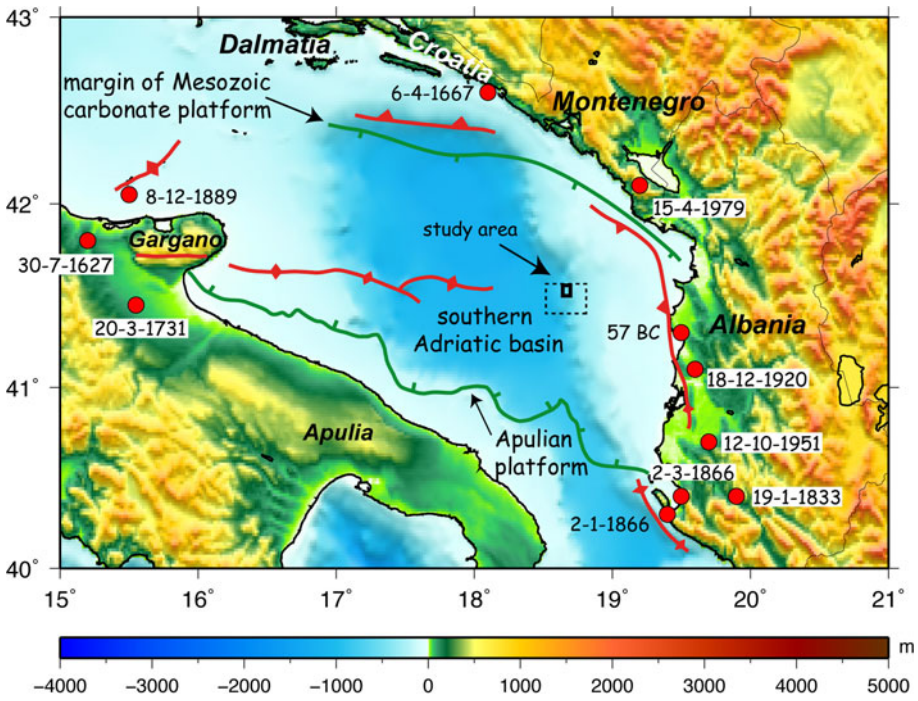

Fig. 1 Map of the southern Adriatic basin with the location of the study area. The main structural elements and the distribution of the sources of historical tsunamis, based on the tsunami catalogue by Tinti et al. (2001), are also shown. The margin of the Mesozoic carbonate platform is indicated in *green*, whereas thrusts and folds are indicated in *red*, with *triangles* and *diamonds*, respectively. The *dashed box* around the study area is the location of Fig. 2. All tsunami-generating events had tectonic origin

Geological setting

The southern Adriatic basin is the current foredeep of the Albanide fold-and-thrust belt (De Alteriis 1995; Argnani et al. 1996; Bertotti et al. 2001) that runs along the eastern boundary of the Adriatic basin.

The southern Adriatic basin is superposed to a Mesozoic epicontinental basin which is bounded to the north and south by Mesozoic shallow-water carbonate platforms, the Dalmatian and Apulian platforms, respectively (Argnani et al. 1996), and this partly explains its anomalous topographic depression within the shallow Adriatic Sea.

The thrust front presents a marked variation in structural style from north to south (Fig. 1). In the northern sector, offshore south Croatia, the topographic boundary of the foredeep basin is mainly given by the WNW-trending margin of the Mesozoic carbonate platform, which is unaffected by the Dinarides thrust front, located in a more internal position. In the Montenegro-Albania sector a large-scale backthrust involves a 5–6 km thick Neogene clastic sedimentary succession that belongs to the thick foredeep basin fill (Argnani et al. 1996). Conversely, the thrust front in the southern part of Albania is characterised by a broad thrust-related fold that affects Mesozoic platform carbonates.

The eastern slope of the southern Adriatic basin has originated by a thick stack of sedimentary prograding units, fed by sediments coming from the adjacent fold-and-thrust belt. Because of the combined contribution of foredeep subsidence and Late Quaternary sea level fluctuations, the shelf edge is now relict, with sediments currently stored at the Albanian coastline. Besides being not fed by sediments carried by the Albanian rivers, the eastern Adriatic slope presents extensive evidence of rather large-scale mass wasting throughout its Late Quaternary evolution (Argnani et al. 2006). This slope, therefore, can be defined as a destructive slope system affected by progressive retreat, which is mainly due to mass-wasting processes, according to the concepts of Galloway (1998).

With respect to the stability of the southern Adriatic slope, it is worth mentioning that although the W-verging Dinaride-Albanide fold-and-thrust-belt runs along the eastern boundary of Adriatic domain, it is from southern Croatia to the south that both geological data and intense seismic activity indicate that this fold-and-thrust belt is currently deforming and tectonically active (e.g. Vannucci et al. 2004). In fact, a large number of earthquakes characterize the southern part of the Dinarides thrust front, in places with large magnitude events (e.g. 1979 Montenegro, $M = 6.8$), and with focal mechanisms showing dominant thrust solutions. The close proximity of the eastern slope of the southern Adriatic basin to a seismogenic region can likely contribute to destabilize the slope sediments. On the other hand, seismicity is almost absent along the coast of Apulia, where earthquakes of low to moderate magnitude occur only in the Gargano Promontory and extend to the NE towards the Tremiti Island; the 1627 tsunamigenic earthquake was likely originated in this region (Tinti and Armigliato 2003).

The eastern slope of the southern Adriatic

Data

In order to investigate the morphology of the eastern slope of the southern Adriatic basin, the SADRI 2005 multibeam survey was carried out on board of R/V Urania, using the system RESON Seabat 8160 which is characterized by 126 beams, spaced 1.2° with a coverage of 150°, and has an operation frequency of 50 kHz. Positioning was achieved by a DGPS Satellite link, and the navigation system PDS-2000 (RESON) was used for multibeam data acquisition. Cruise speed was on average 7 knots.

Multibeam data have been processed using the multibeam-manager software by PANGEA. Sub-bottom profiles data were acquired during the multibeam survey by a 16 transducers hull-mounted DATASONICS CHIRP-II profiler, with operating frequencies ranging between 2 and 7 kHz, in order to investigate the internal structures of sub-bottom sediments (e.g., Damuth 1980).

Morphology of the eastern slope of the southern Adriatic Basin

Swath bathymetry shows that the eastern slope of the South Adriatic basin is incised by a large number of scars of variable size that are not connected to a drainage system (Fig. 2). These erosional features are likely originated by submarine landslides.

The age of the landslide events is difficult to assess, although some brackets can be put considering the stratigraphic architecture of the slope. The eastern slope of the Adriatic basin is the final slope of a prograding set that was likely deposited during the last sea-level lowering (about 22–24 ka BP; Waelbroeck et al. 2002). Therefore, the landsliding events that affected the slope may have originated either at the maximum lowstand or during the subsequent sea-level rise.

Slope failures are expected to occur during maximum sea-level lowstand (Posamentier and Vail 1988) and slide deposits attributed to the last sea-level lowstand are widely reported in the Mediterranean (e.g., Nisbet and Piper 1998; Rothwell et al. 1998; Reeder et al. 2000). However, given the remarkable seismic activity of the adjacent thrust front, it is not unreasonable to assume that slope failure has continued till present. The abundant scalloped features present along the slope (Fig. 2) suggest repeated events of retrogressive landsliding that possibly initiated during the last sea-level lowstand and then continued till present.

One of these submarine slides has been investigated in detail: its geomorphological characteristics and the assessment of its tsunamigenic potential are discussed in the following sections.

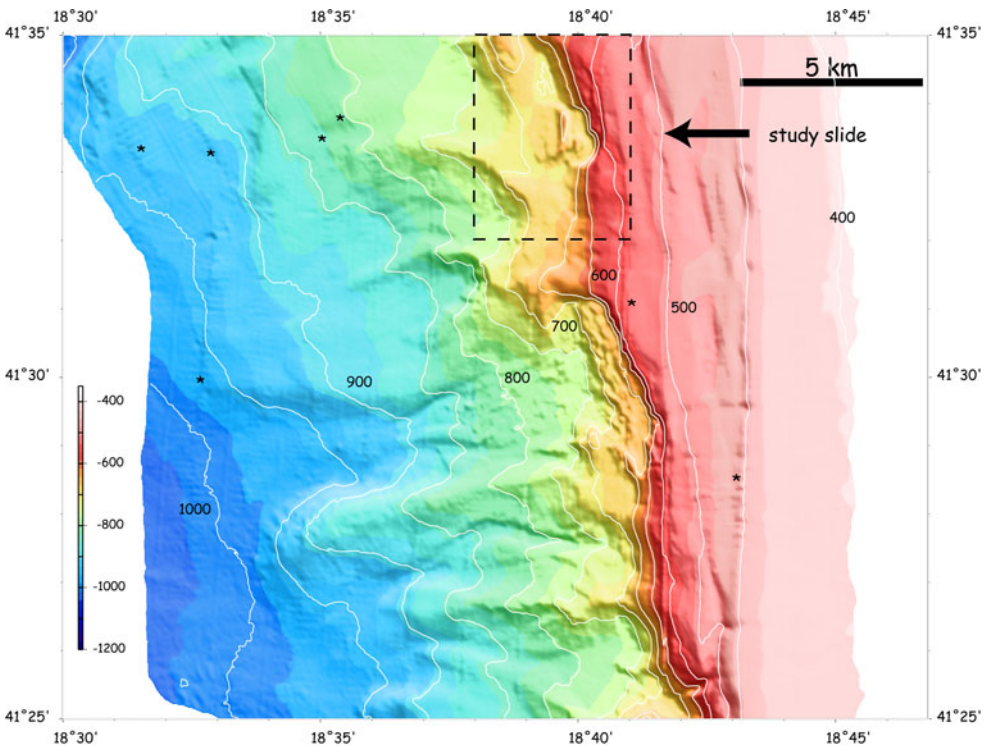

Fig. 2 Multibeam *shaded* relief of a sector of the eastern slope of the southern Adriatic basin where the study area is located (*dashed box* indicating Fig. 3). The slope shows abundant scalloped features, suggesting repeated events of retrogressive landsliding. Note that the studied slide is just one of the smallest slide events, with only limited displacement of material from its original position. Isobaths in m, spaced 50 m, are indicated with *white lines*, and marked every 100 m. The main artefacts due to ship tracks are indicated by a *star*

The slide

The studied landslide is relatively small, and its headscarp is at a water depth of ca. 560 m within the eastern southern Adriatic slope (Fig. 3).

The slide is located at the southern end of a larger slide headscarp, positioned at the shelf edge (Fig. 2), appearing to be the last episode in a process of retrogressive sliding.

The slide headscarp is quite sharp and rather steep (up to 20°), dissecting a fairly regular slope, about 9° steep, which trends ca. N–S (Fig. 3). The sea floor at the base of the slope is rather flat at a depth of about 700 m, except in front of the slide scar, where a mounded region is present. A remarkable N–S-trending steep ridge sticks out from this mounded area by about 50 m. A smaller, subcircular relief is located to the east of the ridge, in the southern part of the mounded area; this secondary relief corresponds to a re-entrance in the southern part of the headscarp. The saddle between the ridge and the subcircular relief is imaged as a mound in the slope-parallel chirp profile (Fig. 4b). These pieces of evidence suggest that the mounded area with its relieves represents the mass slid from the adjacent slope scar (Fig. 3).

The slide deposit reaches a water depth of ca. 700 m and is composed by sediments that show only minor internal disruption. The displacement is limited, in the order of about 1 km, as inferred from the bathymetric map (Fig. 3), allowing a good comparison between volume of displaced material and volume of the scar and evacuation zone. In fact, by using chirp sonar data (Fig. 4) and detailed bathymetry, these volumes can be estimated with an acceptable accuracy. Because of these characteristics, this

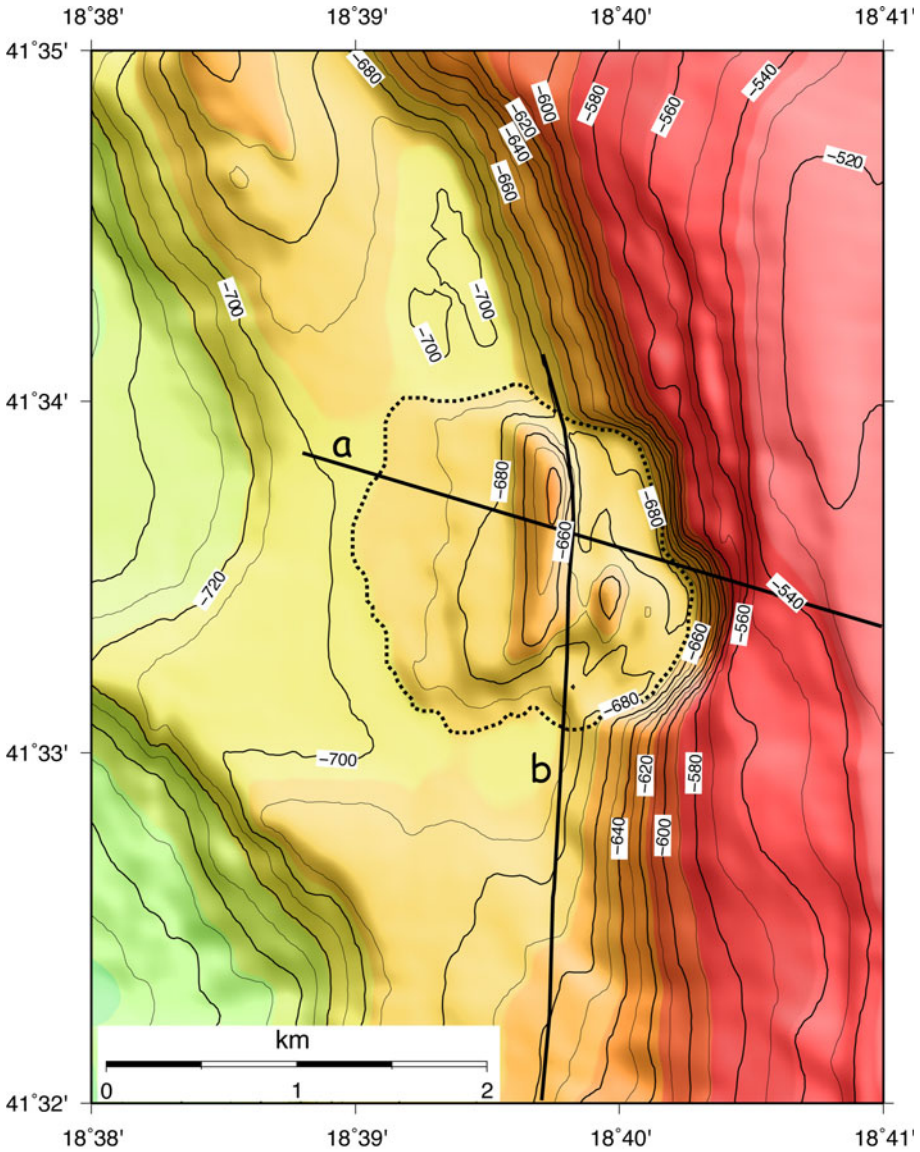

Fig. 3 Detail of multibeam bathymetry in the study area (located in Fig. 2) showing the morphology of the slide, and imaging the slide heardscarp and slide deposit (bounded by the *dashed line*). Note the steep N–S ridge that sticks out from the slide deposits, and the subcircular relief located to the SE of the ridge. The ideal eastern envelope of these two relieves mimics the shape of the headscarp. The traces of two chirp sonar profiles crossing the slide deposit are also indicated

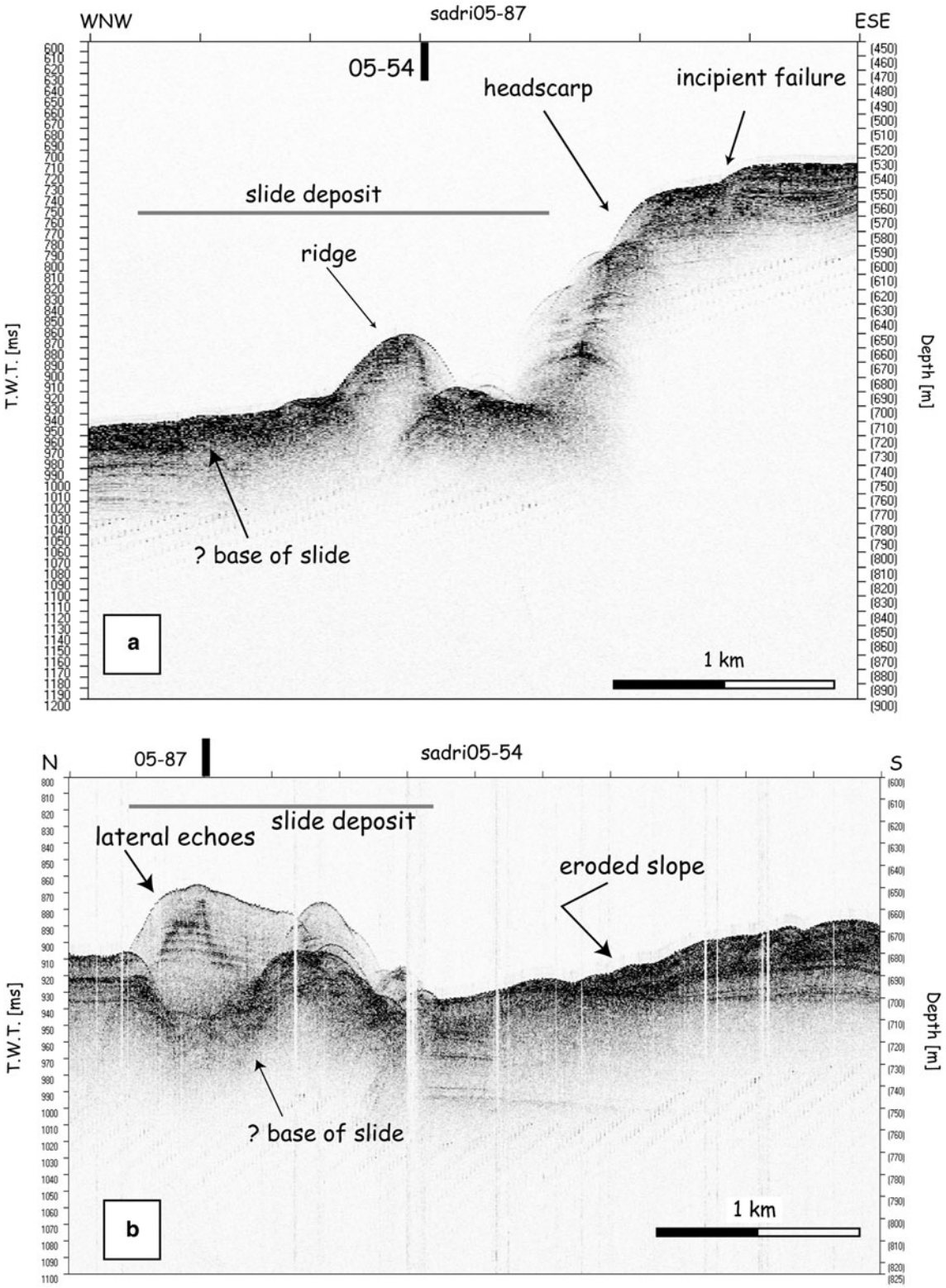

Fig. 4 Chirp sonar profiles crossing the studied slide. Upper panel **a** downslope profile showing the headscarp and slide deposit. Note the steep and narrow ridge that sticks out from the slide deposit. VE is ca. ×6. Lower panel **b** transversal profile crossing the slide deposit and showing the adjacent eroded slope. The mound below the echoes is the saddle between the ridge and the subcircular relief of Fig. 3, whereas the small trough to the north represents the boundary of the slide deposit. VE is ca. ×11

slide has been selected to test some of the expedite methods that are used in the literature to calculate landslide volume from the scar features (e.g., McEwen 1989; McAdoo et al. 2000).

Estimate of the landslide volume

In order to compute the volume of the landslide scar we have reconstructed the pre-slide topography using the adjacent isobaths as a guide, i.e. we are assuming an initial regular slope. Then, by using a set of detailed slope-perpendicular bathymetric profiles, spaced from about 150–500 m, and covering the slide scar and the adjacent slope, we subtracted the post-slide from the pre-slide topography to obtain the area of the evacuated material along the profile. By summing these areas through the serial profiles we obtained an evacuated volume of 0.031 km^3.

The volume of the landslide deposit has been computed by using the same approach of reconstructing a pre-slide topography. Through several detailed topographic profiles the volume of the deposits results to be of about 0.023 km^3. About 26% of the material is therefore missing. However, allowing the uncertainties in computation and the fact that some sediments may have escaped by transformation into turbidites or other gravity flows, the comparison between volume of the scar and volume of the deposit can be considered satisfactory, and in agreement with the limited displacement that is observed.

In their general occurrence, landslides show much larger displacement and materials of the slid mass are often transformed into a variety of gravity flows (e.g. Coleman and Prior 1988; Hampton et al. 1996; Mulder and Cochonat 1996; Canals et al. 2004), making the reconstruction of the volume of the deposit of a specific landslide episode very difficult, if not impossible. Because of these difficulties, landslide volume is often estimated by using the volume of the scar, within the assumption that such scar has been originated by a single evacuation episode. Moreover, the topographic details (or the time available) do not always allow to apply the relatively time-consuming approach that we used for our study landslide, and some approximate geometric descriptions are often adopted to calculate landslide scar volumes.

Two methods, widely used in the literature, have been applied to our study slide, in order to estimate the volume of the scar (Fig. 5). The results are here compared to the more accurate estimates obtained from the serial topographic profiles.

The first method comes from studies on landslides mapped on the rocky planets of the solar system, where they have been investigated using radar imagery. The

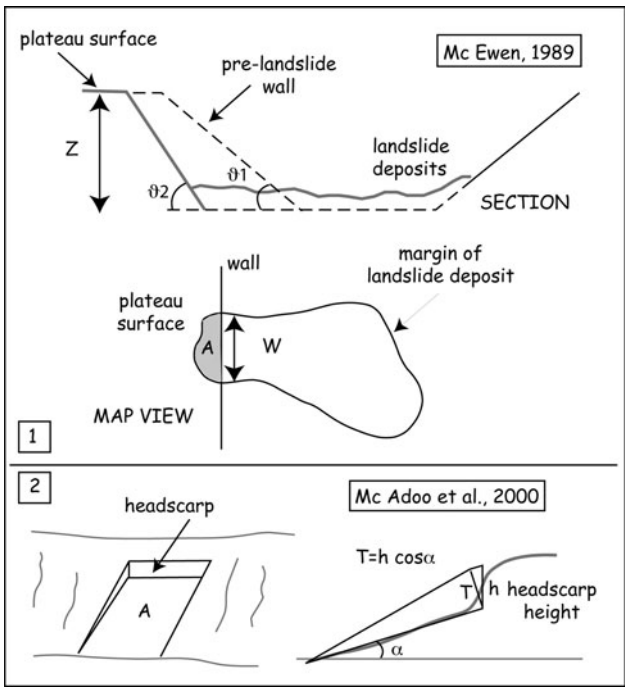

Fig. 5 Schematic diagrams showing two approximate methods for slide volume estimate from detailed DTM. Both methods aim at calculating the material removed from the slide scar (see text). (*1*) W = width of scarp embayment, Z = elevation between plateau surface and canyon floor, A = surface area of material removed by landslide (after McEwen 1989). (*2*) T = thickness related to headscarp height, A = area of the scar (from McAdoo et al. 2000)

volume of Martian landslides has been estimated by using the following analytical relationship (McEwen 1989):

$$V = AZ + 0.5WZ^2[\tan(90^\circ - \theta_1) - \tan(90^\circ - \theta_2)]$$

where Z is the difference in elevation between the top and the base of the scar, A is the area of the upper surface removed by the slide, W is the width of the scarp embayment, θ_1 is the estimated pre-landslide slope, and θ_2 is the post-landslide slope. We applied this method to our study landslide, with the following parameters: Z = 0.090 km, A = 0.257 km^2, W = 1.607 km, $\theta_1 = 9°$, $\theta_2 = 22°$. The resulting volume is of about 0.042 km^3, i.e., overestimating by about 35% our best estimate.

The second method we adopted has been used to analyze the volume of a large number of landslides along the whole of the US continental margins (McAdoo et al. 2000). In this expedite approach the landslide scar is represented as a wedge-shaped volume (approximated by a triangle), which is described by the following relationship:

$$V = 0.5AT$$

where A is the area of the scar and T = (h cos α) is the thickness, with h being the headscarp height and α being the scar slope angle.

For our study slide, $\alpha = 0°$, h = 0.09 km, and A = 0.62 km^2, resulting in a volume of about 0.028 km^3, which underestimates by about 10% our accurate estimate.

To summarize, expedite methods, which often represent the only possible approach, can under- or over-estimate landslide volume by a large percent. The method developed by McAdoo et al. (2000), however, gives a reasonable approximation for the case presented here.

Tsunamigenic potential assessment

Based on the information contained in tsunami catalogues (e.g. Tinti et al. 2001 for the Euro-Mediterranean region, Tinti et al. 2004 for Italy), the southern Adriatic region can be considered as exposed to low-to-moderate tsunami hazard. The distribution of the historical seismic events responsible for tsunamis (Fig. 1) shows that on the western side of the basin the Gargano peninsula is the area most exposed to near-field tsunami attacks, while in the eastern side the southern Dalmatian and the Albanian coastlines show a non-negligible exposure. It is worth noticing that all the events contained in the catalogue have tectonic origin. Moreover, few of them have a tsunami intensity value assigned, the largest (5 in the Sieberg-Ambraseys scale) being relative to the 30 July 1627 tsunami in Gargano and to the 18 December 1920 tsunami in Albania.

The landslide considered in the present study has a small volume (0.031 km^3) and has been mapped in deep waters (560–700 m), which implies that we do not expect a significant tsunamigenic potential. Since the dating of the deposit is not constrained, we can consider two distinct scenarios corresponding to the end members of the landslide occurring (1) at the time of the last glacial maximum (ca. 20–24 ka BP; Waelbroeck et al. 2002) and (2) at present. The main difference between the two scenarios consists in the position of the shoreline and hence in the bathymetry of the considered domain, the paleo-sea-level being decreased by about 137 m with respect to the present sea level (Fairbanks 1989; Waelbroeck et al. 2002). As for the methodology, we first simulate the landslide motion and then we provide the results as inputs for the tsunami propagation simulation.

Landslide simulation

The landslide simulation has been performed by using the UBO-BLOCK2 code, developed by the University of Bologna Tsunami Research Team. The code is the extension to 2D of a code originally developed in 1D (Tinti et al. 1997). Both versions of the code have been extensively applied to several cases of tsunamigenic landslides (e.g. Tinti et al. 2003, 2006). The model is Lagrangian: the sliding mass is split into a 2D matrix of interacting blocks, which can deform while conserving their volume. The equations are solved for the centre of mass of these blocks. All relevant details on the model are provided for example in Tinti et al. (2006).

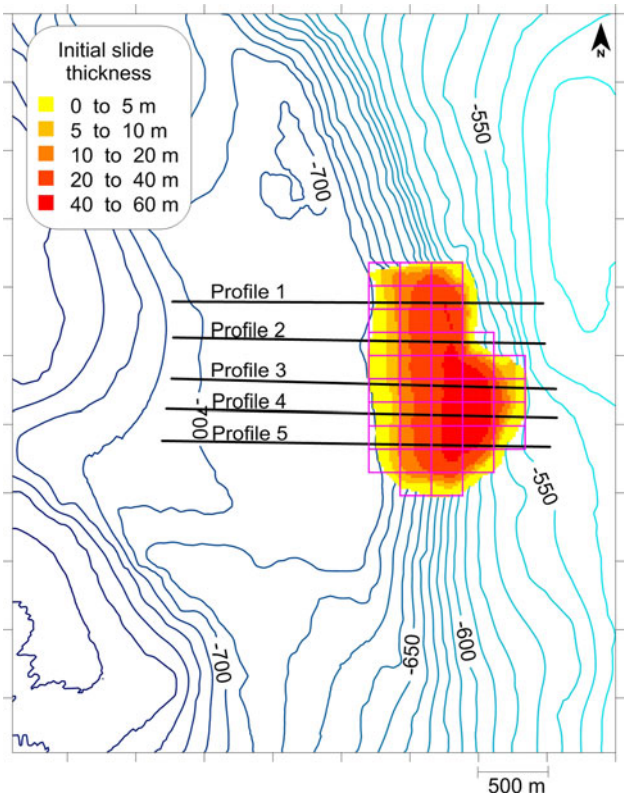

Fig. 6 Reconstructed initial position and thickness of the studied landslide superimposed on the present day bathymetry. The five *black lines* indicate the profiles along which the results of the landslide motion simulation are shown (see Fig. 7). The reticulate in *purple* represents the discretisation in blocks used in our modelling (39 blocks)

The initial sliding mass position and thickness have been reconstructed based on the bathymetric survey data and on the estimate of about 0.031 km^3 for the evacuated volume (Fig. 6). The discretisation in blocks of the initial body is indicated in purple in Fig. 6. Observing that the final deposit lies on a region of very flat bathymetry (see the area delimited by the 700-m isobath in Fig. 3), we can make the assumption that the base of the slide deposit is flat and horizontal. We compare the results of the simulations in terms of position and thickness of the final deposit with the observations along the five different profiles shown in Fig. 6. The results are displayed in Fig. 7. Red lines represent the profile of the simulated sliding mass, which approximates quite well the final position, but not accurately the final body shape, especially for profiles 1 and 2. These two profiles cross the portion of the slide with lower

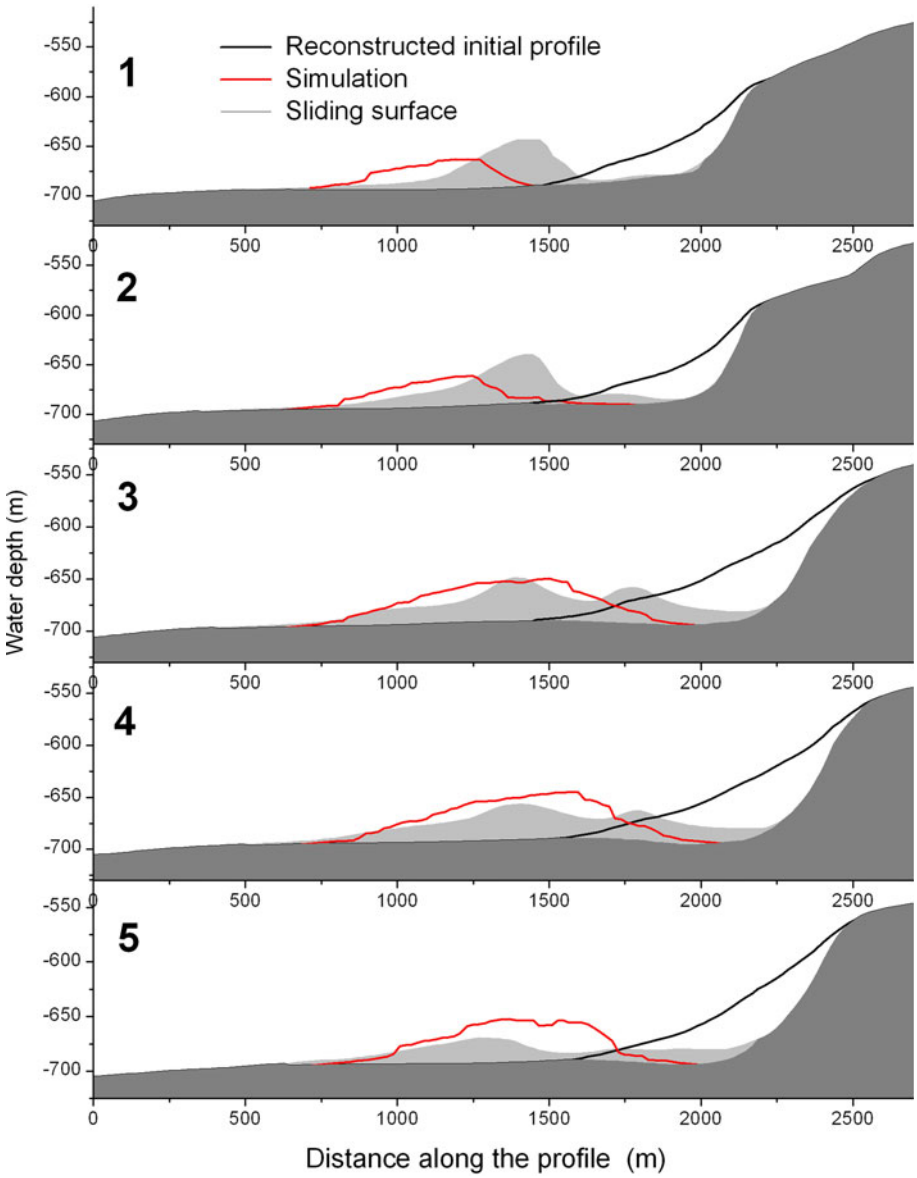

Fig. 7 Results of the landslide simulations along the five profiles plotted in Fig. 6. The observed deposit is represented in *light grey*. The scar geometry in the model reproduces the observed one, while the assumption of a flat and horizontal deposit basement is justified by the flat bathymetry found around the 700 m isobaths

thickness. The difference between the observed and simulated results can be due to different factors. The first may be related to the block discretization we adopted, with the peripheral blocks possibly poorly modelling the real slide motion in that sector. More generally, real landslides can experience several types of changes during their motion, including phase changes in the sliding mass, which cannot be fully treated by our model. But this does not represent a problem from the perspective of the tsunami generation potential, which is attained in the very first seconds of the landslide motion. Figure 8 shows the evolution of each centre of mass velocity with time: a maximum value of around 12 m/s is reached for some blocks, with the average velocity (red line) attaining a similar top value (around 11 m/s). The maximum velocities are reached by the blocks located at the rear of the slide.

As can be deduced from the literature, the range of the typical velocities obtained as the result of numerical modelling of submarine landslides is quite large, depending on a number of factors including the type of landslide (translational or rotational, which in turn determines the extent of horizontal movement), the volume involved, the rheology of the material forming the sliding body, the bathymetric gradient of the sliding surface and so on. For example, Tinti et al. (2006) obtained maximum velocities around 35 m/s for the main submarine landslide occurred in Stromboli (southern Italy) on 30 December 2002: this landslide was composed of volcanic material, had a translational motion and occurred on steep bathymetric gradients, at least in the first part of its motion. As another example Lastras et al. (2005) simulated the BIG'95 debris flow (western Mediterranean) through a complex rheology

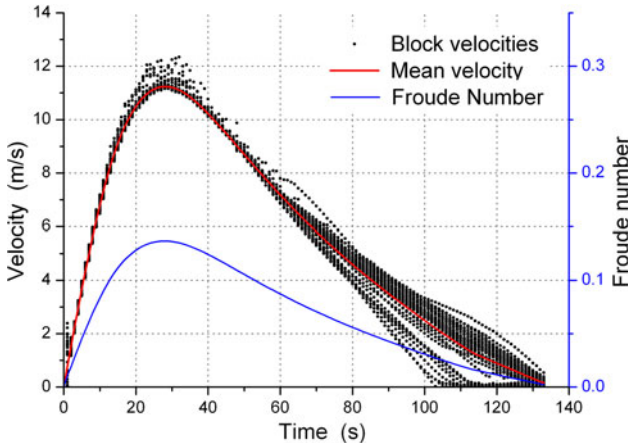

Fig. 8 Individual block velocities and mean velocity (scale on the *left side*), and Froude number (scale on the *right side*) resulting from the landslide motion simulation

model involving a mobile part as well as blocks, representing respectively the loose material and the cohesive sediments. The maximum velocities obtained in that study were of about 50 m/s for the mobile part and 24 m/s for the solid blocks.

The low velocities obtained in our case appear to be coherent with the slump nature of the landslide, the limited fall height (about 100 m) and the relatively small volume. Combined with the considerable depth at which the landslide moves (600–700 m), these factors lead to predict a reduced tsunami generating potential. This can also be deduced from the Froude number graph (blue line in Fig. 8), where the peak value of ca. 0.14 is well below the critical value of 1. It is recalled here that the Froude number is defined as the ratio between the horizontal component of the velocity of the slide and the phase velocity of the tsunami. It represents a measure of the capability of a landslide to generate tsunamis: the closer the Froude number is to 1, the more efficient is the process of energy transmission from the sliding mass to the water waves.

Tsunami simulation

The wave generation and propagation is computed via the UBO-TSUFD code, developed by the University of Bologna Tsunami Research Team. The simulation model solves both linear and non-linear shallow water equations in Cartesian coordinates through a finite-difference leap-frog technique on staggered grids. The code provides also the possibility to work with nested grids. In the non-linear version UBO-TSUFD can compute run-up and inundation, by means of a moving boundary algorithm. UBO-TSUFD successfully passed the so-called "Catalina Island 2004 Benchmark Set" (Liu et al. 2008): the benchmarking was carried out in the framework of the European Commission funded project TRANSFER (http://www.transferproject.eu/). The code has already been applied to a number of cases. For instance, UBO-TSUFD was applied in TRANSFER to the computation of inundation maps in the Messina Straits, southern Italy. Moreover, Tonini et al. (2010) applied the code successfully to the simulation of the tsunami generated by the 29 September 2009 earthquake in Samoa.

In the present application, where we are interested in the gross features of the tsunami propagation, we adopt a coastal boundary acting as a reflecting wall, that is to say that we don't perform any run-up/inundation calculation. Similarly, we employed a single computational grid (no nesting). The way the landslide and the tsunami models are

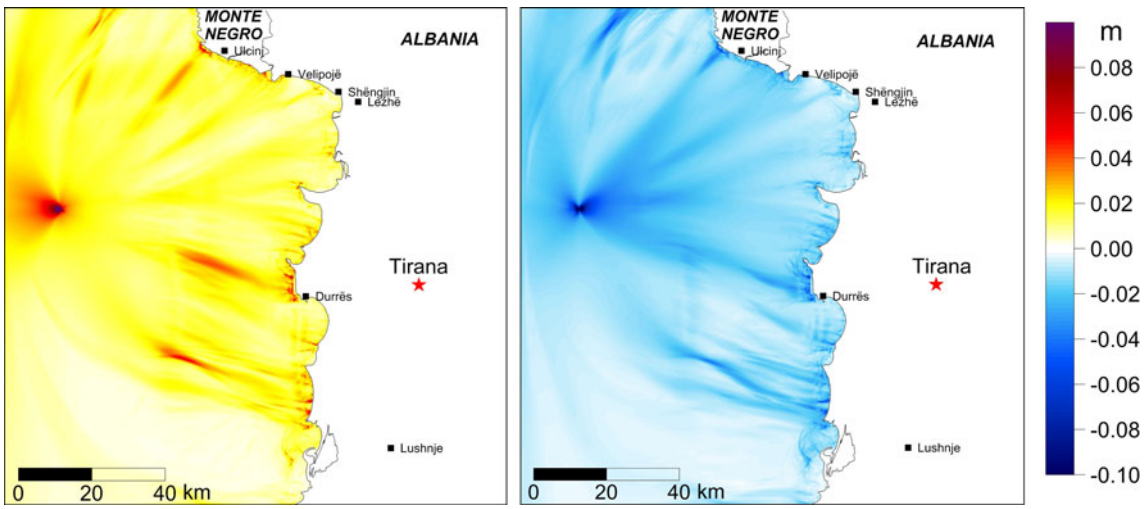

Fig. 9 Maximum positive (*left*) and maximum negative (*right*) water elevation fields computed over a 80 min simulation interval for Scenario 1, corresponding to the present day sea level. Some toponyms are shown for easier geo-referencing

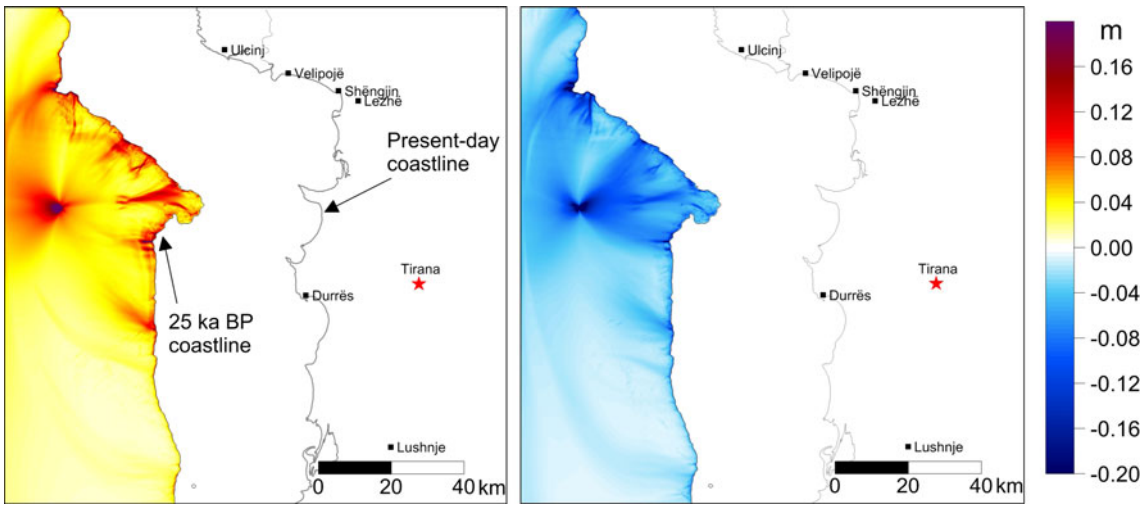

Fig. 10 Maximum positive (*left*) and maximum negative (*right*) water elevation fields computed over a 80 min simulation interval for Scenario 2, corresponding to the 25 ka BP (last glacial maximum) sea level

linked is fully described in Tinti et al. (2006), and the interested reader can refer to that paper for the details.

As previously mentioned, we built two different numerical scenarios. The first (hereafter referred to as Scenario 1) is based on the hypothesis that the landslide is "recent" and hence that it occurred when the bathymetry and coastline position were similar to present. In the second scenario (Scenario 2) we postulate that the landslide occurred in correspondence with the last glacial maximum: adopting the already mentioned value of about 137 m for the difference between the present and the paleo sea levels, we decrease the bathymetry of the domain by the same amount and we coherently change the coastline position and shape. We then adopt two different computational domains, plotted respectively in Figs. 9 and 10. In both cases, the domain is discretised by means of a 80-m resolution grid. Figures 9 and 10 show the pattern of the maximum positive and maximum negative water elevations computed over a 80-min simulation time. The most evident feature is the small value of the computed elevations, not exceeding 10 cm in Scenario 1. In Scenario 2 the tsunami elevation maxima are almost doubled, but still remain modest. The pattern of the fields can be taken as roughly representative of the tsunami energy propagation paths, with a maximum concentrated in the source region and energy beams mostly determined by the interaction of the propagating waves with the seafloor bathymetry.

An example of the evolution of the tsunami over time is provided in Fig. 11 for Scenario 1. The tsunami basically consists in a single wave packet, radiating almost radially from the source and then being slightly distorted by the refraction induced by local bathymetric features. The first tsunami impact on the coast is seen to occur at about 30 min after the landslide initiation, and after about 40 min almost the entire coastline is affected by the tsunami waves. The wave train is characterised by high frequencies, as confirmed also by the synthetic marigrams computed in the six points plotted in red in Fig. 11 and shown in Fig. 12. Point 1 is found close to the source and lies in the open sea for both Scenario 1 and Scenario 2. Points 2 and 3 are in the open sea for Scenario 1, but along the 20–24 ka BP coastline for Scenario 2. Finally, points 4–6 are found on the present-day coastline and no computation is made in these points for Scenario 2.

Though the perturbation reaching the coast is negligible, nonetheless we can stress that some interesting features can be deduced. For example, the first leading signal is negative (apart from point 6), which is a typical characteristic of underwater landslides. The typical period of the tsunami in the open sea (point 1) is around 1 min for both Scenario 1 and Scenario 2, with peak-to-trough amplitude of 5 and 13 cm respectively. It is worth noticing that periods in the order of one to few minutes are comparable to the Eigenperiods of harbours and hence can trigger resonance effects, with the result that even small-amplitude waves like those we found in this study can turn out to be dangerous in specific harbours or small bays. The signals related to Scenario 2 arrive later than for Scenario 1 since the tsunami travels in shallower waters and is then slower. Finally, the coastal records in points 4 and 5 appear as high-frequency, very small amplitude persistent signals, and the result in point 6 is almost null.

Conclusions

The eastern slope of the southern Adriatic basin is dissected by landslide scars and can be characterized as a

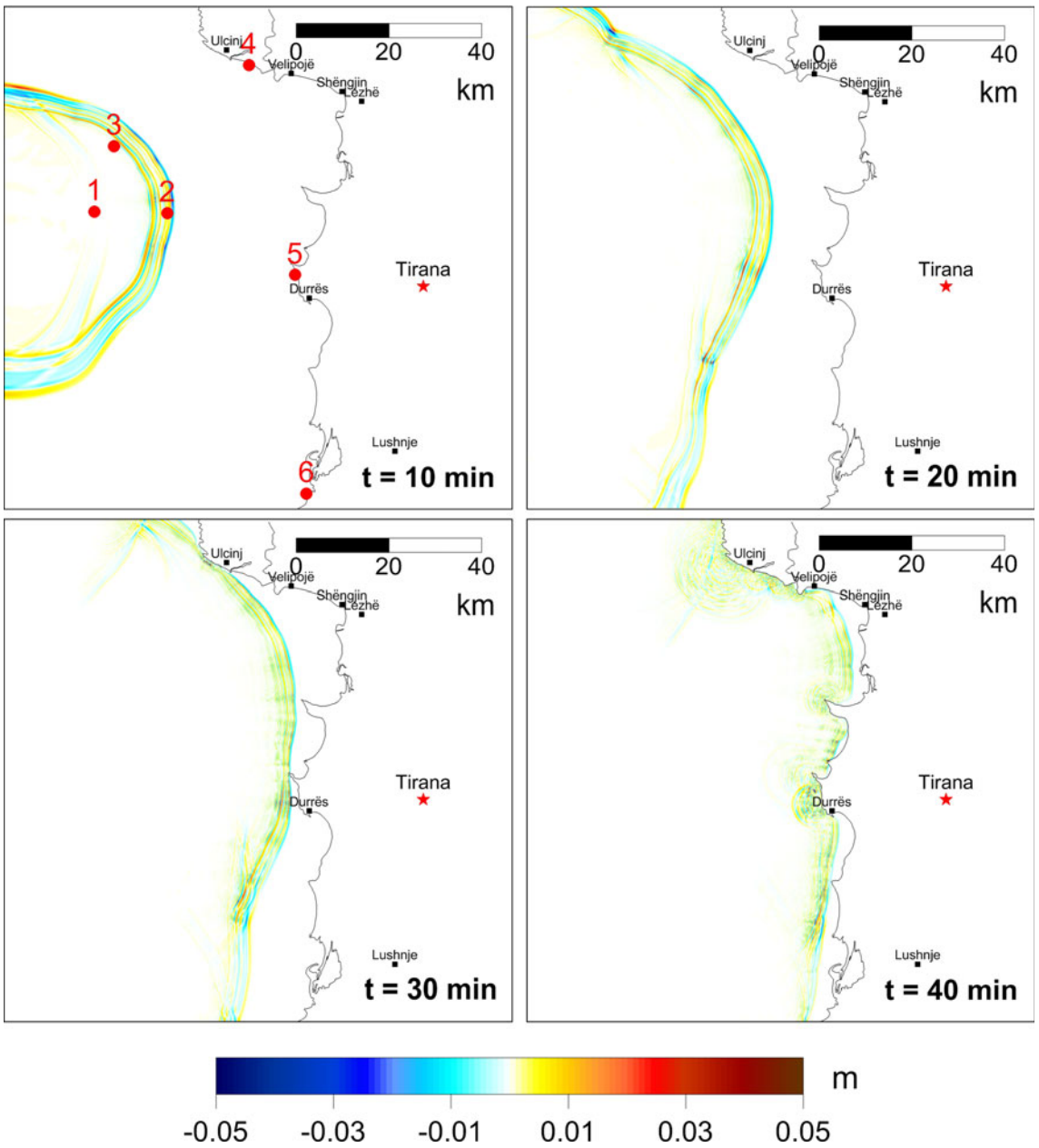

Fig. 11 Snapshots of the tsunami propagation fields computed for Scenario 1. Points numbered 1–6 are the computational nodes where synthetic sea-level time histories have been computed (see Fig. 12)

destructive slope system. One of the landslides has been studied in detail using swath bathymetry and chirp sonar profiles to obtain the volumes of the scar and deposit and the slide displacement. We here remark that because of the poor weather conditions during the survey the quality of the data is far from excellent, but we are confident that it is good enough to support our interpretation, which is also consistent with the overall setting of the eastern southern Adriatic margin. The volume estimates for the scar and deposit are almost comparable, corresponding to about 0.031 and 0.023 km^3, respectively. Displacement is limited and stratal disruption is minimal. Landslide and tsunami modelling suggest that the sliding mass does not produce a significant tsunami on the coasts of the South Adriatic basin whichever the hypothesis on the landslide age is (present vs. 20–24 ka BP sea level). Nevertheless, the case studied in this paper can be taken as a lower case limit for other events that could occur along the scarp. The observed features concerning the generated wave and its impact on the coast (the first signal polarity, the travel time, the spatial distribution of the maximum and minimum elevations) can be considered valid also for bigger landslides,

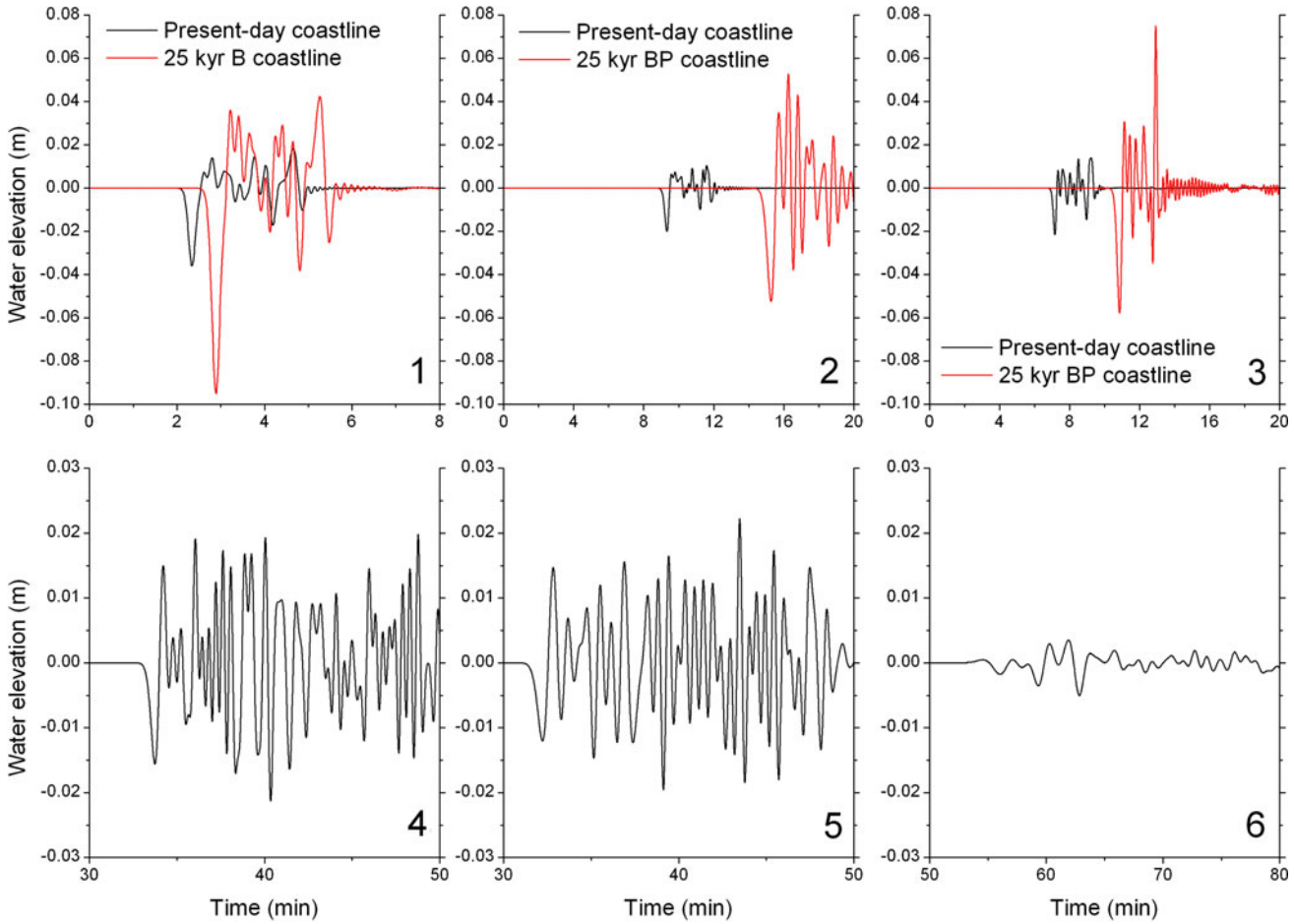

Fig. 12 Synthetic tide-gauge records computed in the six points plotted in Fig. 11. Note that points 2 and 3 lie in the open sea for Scenario 1 and on the coastline for Scenario 2, and that points 4–6 are found along the coastline for Scenario 1, while no computation is made in these points for Scenario 2

providing a useful scenario for the effects of such kind of events.

Acknowledgments A. Argnani and D. Panetta gratefully acknowledge the support of the captain and crews of R/V Urania, and the help given by all the participants in the SADRI 2005 cruise, and by M. Rovere for processing of multibeam data. This study was also partially supported by the EU project TRANSFER (Contract n. 037058 GOCE). The comments of three anonymous referees greatly helped improving the clarity of this contribution.

References

Argnani A, Bonazzi C, Evangelisti D, Favali P, Frugoni F, Gasperini M, Ligi M, Marani M, Mele G (1996) Tettonica dell'Adriatico meridionale. Mem Soc Geol It 51:227–237

Argnani A, Bonazzi C, Rovere M (2006) Tectonics and large-scale mass wasting along the slope of the southern Adriatic basin. Geophys Res Abstr 8:19–20

Bertotti G, Picotti V, Chilovi C, Fantoni R, Merlini S, Mosconi A (2001) Neogene to Quaternary sedimentary basins in the south Adriatic (Central Mediterranean): foredeeps and lithospheric buckling. Tectonics 20:771–787

Canals M, Lastras G, Urgeles R, Casamor JL, Mienert J et al (2004) Slope failure dynamics and impacts from seafloor and shallow sub-seafloor geophysical data: case studies from the COSTA project. Marine Geology 213:9–72

Coleman JM, Prior DB (1988) Mass wasting on continental margins. Ann Rev Earth Planet Sci 16:101–119

Damuth JE (1980) Use of high-frequency (3.5–12 kHz) echograms in the study of near-bottom sedimentation processes in the deep-sea: a review. Mar Geol 38:51–75

De Alteriis G (1995) Different foreland basins in Italy: examples from the central and southern Adriatic Sea. Tectonophys 252:349–373

Fairbanks RG (1989) A 17, 000-year glacio-eustatic sea level record: influence of glacial melting rates on the younger Dryas event and deep-ocean circulation. Nature 432:637–642

Galloway WE (1998) Siliciclastic Slope and Base-of-Slope Depositional systems: component facies, stratigraphic architecture, and classification. AAPG Bull 82:569–595

Hampton M, Lee HJ, Locat J (1996) Submarine landslides. Rev Geophys 34:33–59

Lastras G, De Blasio FV, Canals M, Elverhoi A (2005) Conceptual and numerical modeling of the Big'95 debris flow, Western Mediterranean Sea. J Sediment Res 75:784–797

Liu PLF, Yeh H, Synolakis CE (2008) Benchmark problems. In: Liu PLF, Yeh H, Synolakis CE (eds) Advanced numerical models for simulating tsunami waves and run-up, vol. 10 of advances in coastal and ocean engineering. World Scientific Publishing, Singapore, pp 223–230

McAdoo BG, Pratson LF, Orange DL (2000) Submarine landslide geomorphology, US continental slope. Mar Geol 169:103–136

McEwen A (1989) Mobility of large rock avalanches: evidence from Valles Marineris, Mars. Geology 17:1111–1114

Mulder T, Cochonat P (1996) Classification of offshore mass movements. J Sediment Res 66:43–57

Nisbet EG, Piper DJW (1998) Giant submarine landslides. Nature 392:329–330

Posamentier HW, Vail PR (1988) Eustatic control on clastic deposition, II-sequence and systems trast models. In: Wilgus CK, Hastings BS, Kendall CGSC, Posamentier HW, Ross CA, Van Wagoner JC (eds) Sea-level changes—an integrated approach, vol 42. Soc. Economic Paleontologists and Mineralogists, Spec. Publ, Anaheim, pp 125–154

Reeder MS, Rothwell RG, Stow DAV (2000) Influence of sea level and basin physiography on emplacement of the late Pleistocene Herodotus Basin Megaturbidite, SE Mediterraenan Sea. Mar Petrol Geol 17:199–218

Rothwell RG, Thomson J, Kaehler G (1998) Low-sea-level emplacement of a very large Late Pleistocene 'megaturbidite' in the western Mediterranean Sea. Nature 392:377–380

Tinti S, Armigliato A (2003) The use of scenarios to evaluate the tsunami impact in southern Italy. Mar Geol 199:221–243

Tinti S, Bortolucci E, Vannini C (1997) A block-based theoretical model suited to gravitational sliding. Nat Haz 16:1–28

Tinti S, Maramai A, Graziani L (2001) A new version of the European tsunami catalogue: updating and revision. Nat Haz Earth Sys Sci 1:255–262

Tinti S, Pagnoni G, Zaniboni F, Bortolucci E (2003) Tsunami generation in Stromboli and impact on the south-east Tyrrhenian coasts. Nat Haz Earth Sys Sci 3:299–309

Tinti S, Maramai A, Graziani L (2004) The new catalogue of Italian tsunamis. Nat Haz 33:439–465

Tinti S, Pagnoni G, Zaniboni F (2006) The landslides and tsunamis of the 30th of December 2002 in Stromboli analysed through numerical simulations. Bull Volcanol 68:462–479

Tonini R, Armigliato A, Tinti S (2010) The 29th September 2009 Samoa Islands tsunami: preliminary simulations based on the first focal mechanisms hypotheses and implications on tsunami early warning strategies. Pure Appl Geophys, (accepted)

Vannucci G, Pondrelli S, Argnani A, Morelli A, Gasperini P, Boschi E (2004) An atlas of Mediterranean seismicity. Ann Geophys, Supplement to vol 47(1):247–306

Waelbroeck C, Labeyrie L, Michel E, Duplessy JC, McManus JF, Lambeck K, Balbon E, Labracherie M (2002) Sea-level and deep water temperature changes derived from benthic foraminifera isotopic records. Quat Sci Rev 21:295–305